Inorg. Chem. **2003**, *42*, 2665–2674

Thorium(IV) Complexes of Bidentate Hydroxypyridinonates[1]

Jide Xu, Donald W. Whisenhunt, Jr., Alan C. Veeck, Linda C. Uhlir, and Kenneth N. Raymond*

Department of Chemistry and Chemical Sciences Division, Lawrence Berkeley National Laboratory, University of California, Berkeley, California 94720-1460

Received August 29, 2002

The coordination chemistry of actinide(IV) ions with hydroxypyridinone ligands has been initially explored by examining the complexation of Th(IV) ion with bidentate PR-1,2-HOPO (H**L**[1]), PR-Me-3,2-HOPO (H**L**[2]), and PR-3,4-HOPO-N (H**L**[3]) ligands. The complexes Th(**L**[1])$_4$, Th(**L**[2])$_4$, and Th(**L**[3])$_4$ were prepared in methanol solution from Th(acac)$_4$ and the corresponding ligand. Single-crystal X-ray diffraction analyses are reported for the free ligand PR-Me-3,2-HOPO (H**L**[2]) [$P\bar{1}$, $Z = 8$, $a = 8.1492(7)$ Å, $b = 11.1260(9)$ Å, $c = 23.402(2)$ Å, $\alpha = 87.569(1)°$, $\beta = 86.592(1)°$, $\gamma = 87.480(1)°$], and the complex Th(**L**[2])$_4$·H$_2$O [*Pna*2$_1$ (No. 33), $Z = 4$, $a = 17.1250(5)$ Å, $b = 12.3036(7)$ Å, $c = 23.880$ (1) Å]. A comparison of the structure of the metal complex Th-PR-Me-3,2-HOPO with that of free ligand PR-Me-3,2-HOPO reveals that the ligand geometry is the same in the free ligand and in the metal complex. Amide hydrogen bonds enhance the rigidity and stability of the complex and demonstrate that the Me-3,2-HOPO ligands are predisposed for metal chelation. Solution thermodynamic studies determined overall formation constants (log β_{140}) for Th(**L**[1])$_4$, Th(**L**[2])$_4$, and Th(**L**[3])$_4$ of 36.0(3), 38.3(3), and 41.8(5), respectively. Species distribution calculations show that the 4:1 metal complex Th(L)$_4$ is the dominant species in the acidic range (pH < 6) for PR-1,2-HOPO, in weakly acidic to physiological pH range for PR-Me-3,2-HOPO and in the high-pH range (>8) for PR-3,4-HOPO-N. This finding parallels the relative acidity of these structurally related ligands. In the crystal of [Th(**L**[2])$_4$]·H$_2$O, the chiral complex forms an unusual linear coordination polymer composed of linked, alternating enantiomers.

Introduction

Thorium is the most abundant radioactive element in nature.[2,3] It can capture slow neutrons and form ^{233}Th, which converts into the fissionable ^{233}U through two β-decays; thus thorium has been used as nuclear fuel.[2,3] Because of its relatively low radioactivity, Th(IV) is also a surrogate for Pu(IV) in nuclear waste separation studies. At pH 7.4 (physiological pH) thorium salts hydrolyze to form colloidal particles of Th(OH)$_4$. Thorium is a toxic heavy metal; either Th(IV) ion or its hydroxide colloids readily react with in vivo proteins, amino acids, and nucleic acids to form stable complexes which are deposited in the body,[4,5] primarily in the liver, bone and bone marrow, spleen, and kidneys.[5,6]

For some time a goal of this laboratory has been the development of specific sequestering agents for the actinides. Ligands containing hydroxypyridinone chelating units have been shown to be effective in animals for the decorporation of Pu(IV), U(VI), Np(IV), Th(IV), and Am(III).[7−18] There

* Author to whom correspondence should be addressed. E-mail: raymond@socrates.berkeley.edu.

(1) Specific Sequestering Agents for the Actinides. 46. Part 45: Paquet, F.; Montègue, B.; Ansoborlo, E.; Hengé-Napoli, M. H.; Houpert, P.; Durbin, P. W.; Raymond, K. N. *Int. J. Radiat. Biol*. **2000**, *76*, 113−117.

(2) Bailar, J. C., Jr.; Emeleus, H. J.; Nyholm, Sir R.; Troyman-Dickenson, A. F. *Comprehensive Inorganic Chemistry, Vol. 5, Actinides*; Pergamon Press: New York, 1973.

(3) Bagnall, K. W. The Actinide Elements. In *Topics in Inorganic and General Chemistry*; Robinson, P. L., Ed.; Monography 15; Elsevier Publishing Co.: New York, 1972; p 15.

(4) Raymond, K. N. Specific Sequestering Agents for Iron and Actinides. In *Environmental Inorganic Chemistry*; Irgolic, K. J.; Martell, A. E., Eds.; Proceedings, U.S.−Italy International Workshop on Environmental Inorganic Chemistry, San Miniato, Italy, June 5−10, 1983; VCH Publishers: Deerfield Beach, FL, 1985; p 331.

(5) Stradling, G. N.; Gray, S. A.; Pearce, M. J.; Wilson, I.; Moody, J. C.; Burgada, R.; Durbin, P. W.; Raymond, K. N. *Human Exp. Toxicol.* **1995**, *14*, 165−169.

(6) Stradling, G. N.; Hodgson, S. A.; Pearce, M. J. *Radiat. Prot. Dosim.* **1998**, *79*, 445.

(7) Raymond, K. N.; Xu, J. Siderophore-based Hydroxypyridinone Sequestering Agents. In *The Development of Iron Chelators for Clinical Use*; Bergeron, R. G., Brittenham, G. M., Eds.; CRC Press: Boca Raton, FL, 1994; p 307.

(8) Sheppard, L. N. Kontoghiorghes, G. J. *Inorg. Chim. Acta* **1991**, *188*, 17.

(9) White, D. L.; Durbin, P. W.; Jeung, N.; Raymond, K. N. *J. Med. Chem.* **1988**, *31*, 11.

(10) Xu, J.; Raymond, K. N.; Durbin, P. W.; Kullgren, B. *J. Med. Chem.* **1995**, *38*, 2606.

(11) Uhlir, L. C. Ph.D. Thesis, University of California, Berkeley, 1992.

(12) Whisenhunt, D. W., Jr. Ph.D. Thesis, University of California, Berkeley, 1994.

10.1021/ic0259888 CCC: $25.00
Published on Web 03/26/2003

Scheme 1. Syntheses of Bidentate PR-1,2-HOPO (H**L**[1]), PR-Me-3,2-HOPO (H**L**[2]), and PR-3,4-HOPO-N (H**L**[3])[a]

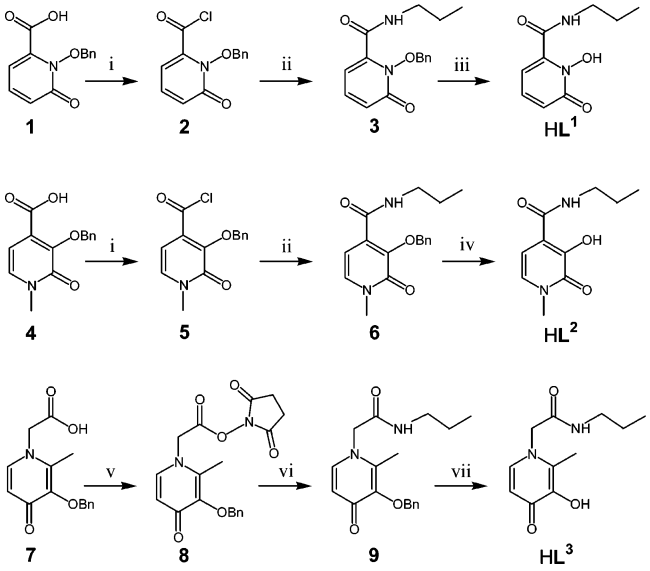

[a] (i) Oxalyl chloride. (ii) *n*-Propylamine, 90%. (iii) HCl/HOAc deprotection, 85%. (iv) H_2, Pd/C, 92−94%. (v) NHS, DCC. (vi) Propylamine, 60.6%. (vii) H_2, Pd/C, 87%.

are three isomers of hydroxypyridinones: 1-hydroxy-2(1*H*)-pyridinone, 3-hydroxy-2(1*H*)-pyridinone, and 3-hydroxy-4(1*H*)-pyridinone, abbreviated here as 1,2-HOPO, 3,2-HOPO, and 3,4-HOPO, respectively. Similar to catechol, the HOPO isomers are highly selective for "hard" metal ions with large charge/radius ratios, such as Fe(III) and Pu(IV). The HOPO monoanions have zwitterionic resonance forms that are isoelectronic with the catechol dianion.[7] While all of these ligands are expected to be monoprotic anions that form stable metal complexes at physiological pH, they possess different acidity and different affinity toward binding metal ions due to the differences in their structures. These facts make it possible to selectively sequester certain metal ions under specific conditions. Bidentate ligands have the greatest concentration dependence on their metal sequestration, while multidentate, particularly octadentate, ligands are much more effective ligands at low concentration. In order to attach the HOPO binding units to a suitable molecular backbone to form multidentate ligands, the HOPO binding units must be functionalized to make a point of attachment. An effective way to achieve this functionality is to add to a carboxyl group to the HOPO ring and then form an amide linkage, similar to that for the catecholamide ligands.[7,10]

Scheme 1 shows the representative bidentate HOPO ligands 1-hydroxy-2(1*H*)-pyridinone-6-carboxylic acid propylamide (PR-1,2-HOPO, H**L**[1]), 3-hydroxy-1-methyl-2(1*H*)-pyridinone-4-carboxylic acid propylamide (PR-Me-3,2-HOPO, H**L**[2]), and 2-(3-Hydroxy-2-methyl-4-(1*H*)-pyridinon-1-yl)-*N*-propyl-acetamide (PR-3,4-HOPO-N, H**L**[3]). The structural and solution thermodynamic properties of actinide complexes with these unconstrained, bidentate hydroxypyridinonate ligands form the basis for the design of optimal multidentate actinide sequestering agents. While all three bidentate HOPOs form very stable complexes with Th(IV), the three ligands have different optimal binding pH ranges.

We have recently reported the X-ray crystal structures and solution thermodynamic formation constants of Ce(IV) complexes with a series of Me-3,2-HOPO ligands.[19] It was anticipated that the complexation of Ce(IV) would show parallels with the Th(IV) catecholate system,[20] and other hydroxypyridinonates such as 1,2-HOPO and 3,4-HOPO ligands would show high affinities toward actinide(IV) ions. Here we examine the structural and solution thermodynamic properties of Th(IV) complexes with the three bidentate HOPO ligands mentioned above. While the Ce(IV) complexes are eight coordinate, the X-ray crystal structure of Th(**L**[2])$_4$·H_2O shows that thorium is nine coordinate, and the complex forms an infinite linear coordination polymeric structure. The coordination geometry of Th(IV) has been analyzed using a new application of the previously defined shape parameters.[19]

Results and Discussion

Synthesis. The updated syntheses of H**L**[1], H**L**[2], and H_2**L**[3] are illustrated in Scheme 1. The original synthesis of H**L**[2] involves the reaction of a thiazolide intermediate with *n*-propylamine, for an overall yield of 64%.[10] We report here a new synthesis, in which the benzyl-protected Me-3,2-HOPO acid is converted into an acid chloride, which then is combined in situ with *n*-propylamine to give the benzyl-protected PR-Me-3,2-HOPO. The benzyl group can be removed by hydrogenation to afford H**L**[2] in an overall yield of 90%. Similarly, the original synthesis[9] of H**L**[1] has been revised by using benzyl-protected acid chloride for coupling with propylamine followed by acidic deprotection to give H**L**[1] in ca. 90% yield. Both the Me-3,2-HOPOBn acid chloride and 1,2-HOPOBn acid chloride are versatile precursors; they readily react with primary as well as secondary or aromatic amines to provide corresponding amides in excellent yield, while the 1,2-HOPOBn- or Me-3,2-HOPOBn-thiazolide intermediates give good yields only with primary amines.[10] In the synthesis of PR-3,4-HOPO-N (H**L**[3]), the acid chloride activation of 3,4-HOPOBn-N-acid was not successful. It was found that pyridine is the optimal solvent for preparing activated *N*-hydroxysuccinimide (NHS) ester of 3,4-HOPOBn-N-acid. Without separation, the crude NHS ester was reacted with *n*-propylamine in situ to convert to

(13) Stradling, G. N.; Gray, S. A.; Ellender, M.; Moody, J. C.; Hodgson, A.; Pearce, M.; Wilson, I.; Burgada, R.; Bailly, T. P.; Leroux, Y. G.; El Manouni, D.; Raymond, K. N.; Durbin, P. W. *Int. J. Radiat. Biol.* **1992**, *62*, 487.
(14) Volf, V.; Burgada, R.; Raymond, K. N.; Durbin, P. W. *Int. J. Radiat. Biol*. **1993**, *63*, 785.
(15) Durbin, P. W.; Kullgren, B.; Xu, J.; Raymond, K. N. *Radiat. Prot. Dosim.* **1994**, *53*, 305.
(16) Stradling, G. N.; Gray, S. A.; Pearce, M. J.; Wilson, I.; Moody, J. C.; Burgada, R.; Durbin, P. W.; Raymond, K. N. *Human Exp. Toxicol*. **1995**, *14*, 165.
(17) Xu, J.; Raymond, K. N. *Inorg. Chem.* **1999**, *38*, 308.
(18) Durbin, P. W.; Kullgren, B.; Xu, J.; Raymond, K. N.; Allen, P. G.; Bucher, J. J.; Edelstein, N. M.; Shuh, D. K. *Health Phys.* **1998**, *75*, 34.
(19) Xu, J.; Radkov, E.; Ziegler, M.; Raymond, K. N. *Inorg. Chem*. **2000**, *39*, 4156−4164.
(20) Sofen, S. R.; Cooper S. R.; Raymond, K. N. *Inorg. Chem.* **1979**, *18*, 1611−1616.

Table 1. Protonation Constants and UV Absorbance Data

ligand	species	protonation constants	λ_{max} (nm)	ϵ (M^{-1} cm^{-1})
PR-1,2-HOPO	$(\mathbf{L^1})^-$		341	4100
	$H\mathbf{L^1}$	4.96(2)[a]	305	6300
PR-Me-3,2-HOPO	$(\mathbf{L^2})^-$		350	9000
	$H\mathbf{L^2}$	6.12(1)[a]	321	5500
PR-3,4-HOPO-N	$(\mathbf{L^3})^-$		318	11500
	$H\mathbf{L^3}$	9.47(2)[a]	286	14000
	$(H_2\mathbf{L^3})^+$	3.03(4)[a]	282	7700

[a] The numbers in parentheses are the standard deviations of the values obtained from at least three trials.

benzyl-protected ligand, and the hydrogenation deprotection affords the $H\mathbf{L^3}$ at good yield.

Solution Thermodynamic Studies: Free Ligands. The ligand protonation constants in this work were determined by potentiometric titration. The ligand protonation constants, K_{an}, may be derived from these cumulative constants according to eq 1. Note that this definition describes proton *association* constants. All three ligands were readily soluble

$$K_{an} = \frac{[LH_n]}{[H][LH_{n-1}]} = \frac{\beta_{01n}}{\beta_{01(n-1)}} \quad (1)$$

and colorless in 0.1 M KCl at 1 mM concentration. The potentiometric titrations were carried out from low to high pH (2.5−11) and viceversa. The results are listed in Table 1.

The protonation constants for $H\mathbf{L^1}$ and $H\mathbf{L^2}$ were determined to be $\log K_{a1} = 4.96(2)$ and 6.12(1), respectively. For $\mathbf{L^3}$ the protonation constant was determined to be $\log K_{a1} = 9.47(4)$. In contrast to $H\mathbf{L^1}$ and $H\mathbf{L^2}$, the neutral $H\mathbf{L^3}$ ligand can be further protonated at low pH resulting in a cationic species $(H_2\mathbf{L^3})^+$. The constant determined for this protonation was $\log K_{a2} = 3.03(4)$. The potentiometric titration curve for $H\mathbf{L^2}$ is shown in Figure 2a, while those of $H\mathbf{L^1}$ and $H\mathbf{L^3}$ are shown in Figures S1a and S2a (Supporting Information). Note that the PR-3,4-HOPO-N is significantly more basic than its 1,2- and 3,2-analogues.

Solution Thermodynamic Studies: Thorium(IV) Complexes. For metal−ligand complexation, the conventional cumulative formation constants,[21] β_{pqr}, were defined according to eq 2; note that the ligand is designated as L:

$$p\mathrm{Th}^{4+} + q\mathrm{L}^{m-} + r\mathrm{H}^+ \rightleftharpoons \mathrm{Th}_p\mathrm{L}_q\mathrm{H}_r^{(4p-mq+r)+}$$

$$\beta_{pqr} = \frac{[\mathrm{Th}_p\mathrm{L}_q\mathrm{H}_r]}{[\mathrm{Th}]^p[\mathrm{K}]^q[\mathrm{H}]^r} \quad (2)$$

The determination of the Th(IV) formation constants with these ligands presented a significant challenge, because in all three cases the 1:1 complexes ThL were very stable and do not show appreciable dissociation even at pH 2.1. Typically, in these cases a competition titration is used against a known ligand like EDTA. In this case, however, the spectrophotometric titrations did not yield a clear answer. The competition titrations were difficult to model with the models including mixed-ligand species like Th(EDTA)L$^-$

(21) Silen, L.; Martell, A. E. *Stability Constants of Metal-Ion Complexes*; Alden Press: Oxford, 1971.

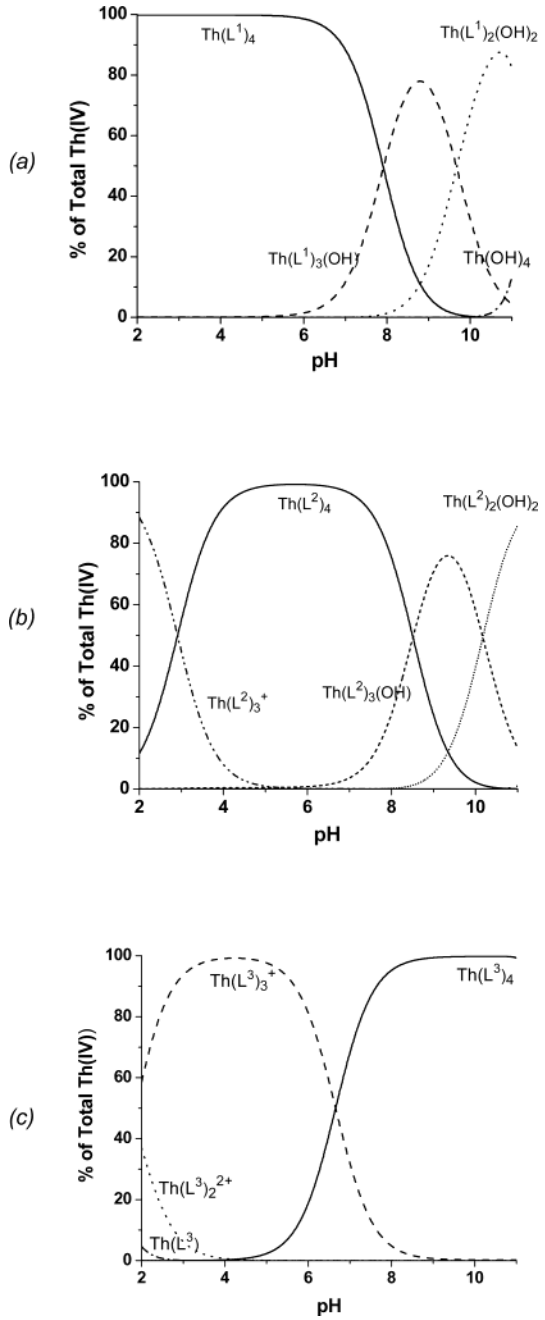

Figure 1. Species distribution of (a) Th(IV)/PR-1,2-HOPO, (b) Th(IV)/PR-Me-3,2-HOPO, and (c) Th(IV)/PR-3,4-HOPO-N systems for solutions containing 1×10^{-4} M Th^{4+} and 1×10^{-3} M ligands.

at low pH. Without the presence of the Th(EDTA) species it was not possible to calculate β_{140}. Additionally, the spectroscopic markers used to monitor this reaction were the UV absorbencies of the protonated ligand, deprotonated ligand, and the ligand coordinated to Th(IV). These transitions are almost entirely ligand based, and therefore the differences in signal in the UV spectra between the deprotonated ligand and the ligand coordinated to Th(IV) are very small.

In order to determine the formation constant β_{140} the titration was carried out at high pH (up to 11). At this pH the formation of $Th(OH)_4$ starts to compete effectively against the $Th(L)_4$, or other partially hydrolyzed complexes, as shown in the species distribution diagrams (Figure 1). Note that the concentration used for the species calculations are

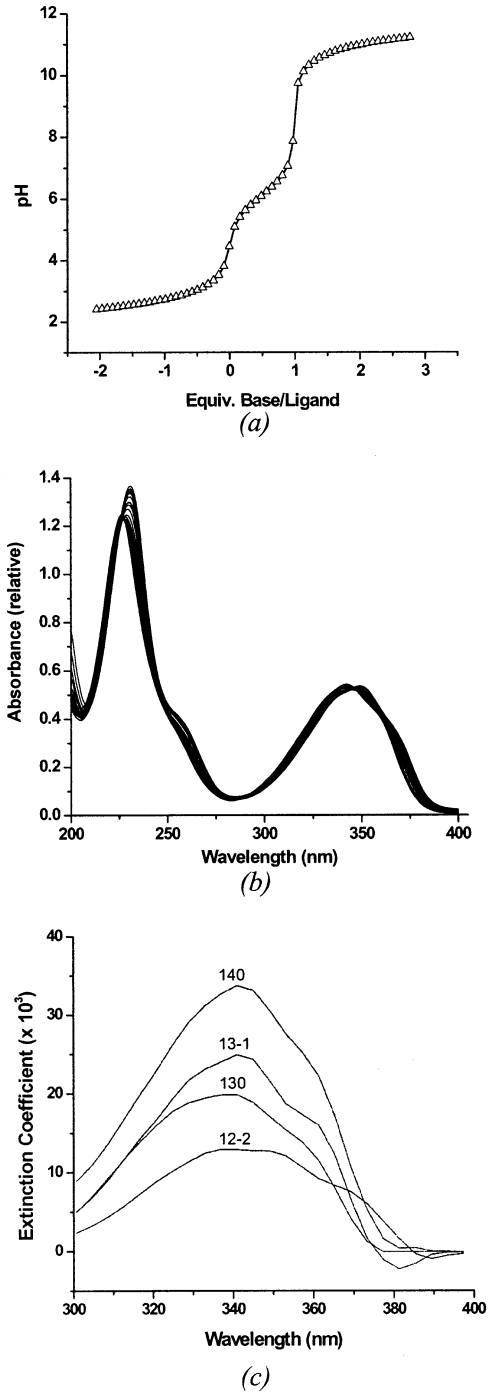

Figure 2. (a) Experimental (open triangles) and calculated (line) potentiometric titration curve of H**L**^{2}. (b) Selected spectra from the spectrophotometric titration of the Th(IV)/H**L**^{2} system. (c) UV/vis absorption spectra of component species $Th_pL_qH_r$ of the Th(IV)/H**L**^{2} system. Spectra are given labels of *pqr*, where a negative value for *r* represents hydroxides bound to Th(IV).

about 1 magnitude higher than that in the practical titration, so the hydrolyses of the thorium complexes are much depressed in these species distribution diagrams. For titrations involving metal−ligand coordination, the constants for the Th(IV) ion hydrolysis species were included as fixed parameters in the refinements.[21] Due to the low solubility of $Th(OH)_4$ it was necessary to carry out the titrations at very low concentration (micromolar) using a cell with 1 cm path length. At this concentration no precipitate was observed at up to 20% (calculated) $Th(OH)_4$. The titrations were run at a 4:1 ligand-to-metal ratio at ~10 μM Th(IV). Attempts to perform this titration at higher concentrations resulted in a white precipitate (presumably $Th(OH)_4$). The titrations were carried out from low pH to high pH. At least 30 data points were collected over the pH range 2.5−11. Before each data point was recorded the pH and spectrum were required to be stable (this generally took 1 h per point as was determined automatically by the data collection system). A single titration could be run in a 48 h period. Under these experimental conditions it was possible to achieve a satisfactory R^2 value (0.004) and satisfactory component spectra.

Table 2. Formation Constants and UV/Vis Absorbance Data for the Th(IV) Complexes

complexation system	*pqr*	log β_{pqr}[a]	λ_{max} (nm)	ϵ (M^{-1} cm^{-1})
Th/PR-1,2-HOPO (H**L**^{1})	140	36.0(3)	318	20000
	13−1	24.9(2)	328	14000
	12−2	12.1(2)	344	10500
Th/PR-Me-3,2-HOPO (H**L**^{2})	140	38.3(3)	344[b]	33300
	130	31.9(3)	344	19700
	13−1	26.6(2)	344	24900
	12−2	13.3(2)	340	12700
Th/PR-3,4-HOPO-N (H**L**^{3})	140	41.8(5)	306[b]	50000
	130	35.8(2)	306	33000
	120	25.0(8)	302	20000
	110	13.5(2)	302	9600

[a] The numbers in parentheses are the standard deviations of at least three duplicate runs. [b] Resolution is ±3 nm.

The models used in fitting the data for the three ligands are similar, and the results are listed in Table 2. For the most acidic ligand H**L**^{1}, no stepwise ligand-to-metal formation constants could be determined. The only species that fit the data involved the complex species loss of ligands through hydrolysis and then finally complete hydrolysis. As with all three titrations the ligand spectra, ligand protonation constants, and thorium hydrolysis constants were held constant. Many models were attempted including those involving $ThL_4(OH)^-$ and dimeric species. In all cases these species did not improve the fit and often led to component spectra that were not reasonable (i.e., negative extinction coefficients). The modeling was very sensitive to the concentration of free deprotonated ligand so those equilibria involving loss of ligand from the metal complexes were easily observed. The relevant equilibria are shown below:

$$Th(\mathbf{L}^{1})_4 + OH^- \rightleftharpoons Th(OH)(\mathbf{L}^{1})_3 + (\mathbf{L}^{1})^-$$

$$Th(OH)(\mathbf{L}^{1})_3 + OH^- \rightleftharpoons Th(OH)_2(\mathbf{L}^{1})_2 + (\mathbf{L}^{1})^-$$

$$Th(OH)_2(\mathbf{L}^{1})_2 + 2OH^- \rightleftharpoons Th(OH)_4 + 2(\mathbf{L}^{1})^-$$

Using the known formation constant for $Th(OH)_4$[22] it was possible to determine the log β_{140} for the $Th(\mathbf{L}^{1})_4$ complex to be 36.0(3) as described in ref 37. The selected spectra

(22) Baes, C. F., Jr.; Mesmer, R. E. *The Hydrolysis of Cations*; John Wiley & Sons: New York, 1976; pp 160−162.
(23) Xu, J.; O'Sullivan, B.; Raymond, K. N. *Inorg. Chem.* **2002**, *41*, 6731−6742.
(24) Garrett, T. M.; Cass, M. E.; Raymond, K. N. *J. Coord. Chem.* **1992**, *25*, 241−253

from the titrations are shown in Figure S1b of the Supporting Information.

The H**L**^{2} ligand is slightly more basic than H**L**^{1}, and therefore it was possible to obtain the $(ThL_3)^+$ to ThL_4 stepwise formation constant at pH 4. The relevant equilibria are shown below:

$$Th(\mathbf{L}^{2})_3^{+} + H\mathbf{L}^{2} \rightleftharpoons Th(\mathbf{L}^{2})_4 + H^+$$

$$Th(\mathbf{L}^{2})_4 + OH^- \rightleftharpoons Th(OH)\,(\mathbf{L}^{2})_3 + (\mathbf{L}^{2})^-$$

$$Th(OH)(\mathbf{L}^{2})_3 + OH^- \rightleftharpoons Th(OH)_2(\mathbf{L}^{2})_2 + (\mathbf{L}^{2})^-$$

$$Th(OH)_2(\mathbf{L}^{2})_2 + 2OH^- \rightleftharpoons Th(OH)_4 + 2(\mathbf{L}^{2})^-$$

Using the known formation constant of $Th(OH)_4$[22] it was possible to determine the log β_{140} as 38.3(3) for the $Th(\mathbf{L}^{2})_4$ complex. The potentiometric titration curve, selected spectra from spectrophotometric titration, and the component spectra for this system are shown in Figure 2a−c. It is interesting to note that the spectra for $Th(\mathbf{L}^{2})_3^{+}$ and $Th(OH)(\mathbf{L}^{2})_3$ are quite similar (Figure 2c), as would be expected due to the electron transition being primarily ligand based; however, the overall charge on the complex appears to slightly affect the shape of the transition. These species, while spectroscopically similar, are present over different pH ranges (see Figure 1b).

The most basic ligand H**L**^{3} formed a very stable $Th(\mathbf{L}^{3})_4$ complex at high pH; the above hydrolysis models for PR-1,2-HOPO and PR-Me-3,2-HOPO complexes are not applicable. The best model for this system included a number of ligand-to-metal stepwise formation constants followed by complete hydrolysis at high pH. This is not surprising due to the high basicity of the ligand. The relevant equilibria are shown below:

$$Th(\mathbf{L}^{3})^{3+} + H_2(\mathbf{L}^{3})^{+} \rightleftharpoons Th(\mathbf{L}^{3})_2^{2+} + 2H^+$$

$$Th(\mathbf{L}^{3})_2^{2+} + H_2(\mathbf{L}^{3})^{+} \rightleftharpoons Th(\mathbf{L}^{3})_3^{+} + 2H^+$$

$$Th(\mathbf{L}^{3})_3^{+} + H\mathbf{L}^{3} \rightleftharpoons Th(\mathbf{L}^{3})_4 + H^+$$

$$Th(\mathbf{L}^{3})_4 + 4OH^- \rightleftharpoons Th(OH)_4 + 4(\mathbf{L}^{3})^-$$

The selected spectra from spectrophotometric titration and component spectra are shown in Figure S2b,c of the Supporting Information. Using the known formation constant of $Th(OH)_4$[22] it was possible to determine log β_{140} to be 38.3(3) for the $Th(\mathbf{L}^{3})_4$ complex.

For H**L**^{1} and H**L**^{2} the complexation equilibria at high pH included a hydrolysis step with loss of a ligand. From the crystal structure of $Th(\mathbf{L}^{2})_4 \cdot H_2O$ (Figure 4) the complex is nine coordinate with an amide oxygen atom taking up the ninth coordination site. This coordinate amide group is displaced by a water molecule when in water. It is proposed that the exchange of hydroxyl ion with this bound water at high pH ultimately leads to the hydrolysis of the thorium ion.

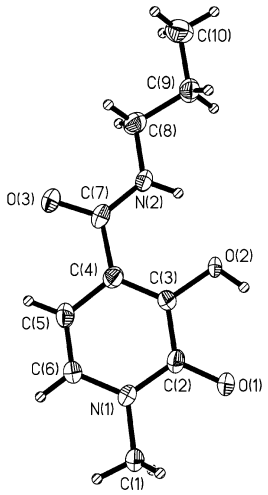

Figure 3. ORTEP view of the structure of the free ligand H**L**^{2}, showing the atom-labeling scheme and 50% thermal ellipsoid probabilities. Note that the hydrogen-bonding mode is typical for hydroxypyridinone ligands.

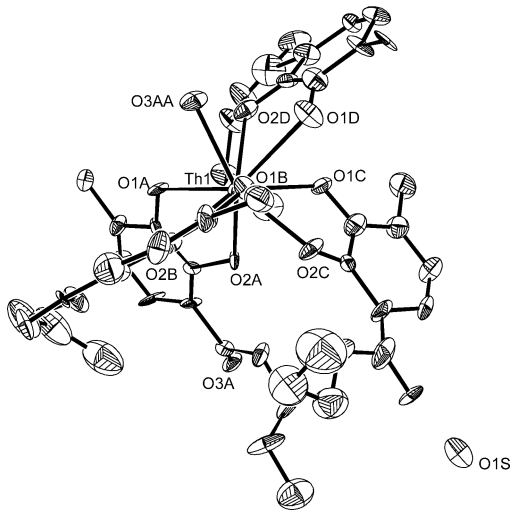

Figure 4. View of the structure of $[Th(\mathbf{L}^{2})]\cdot H_2O$, showing the atom-labeling scheme of the oxygen atoms and 30% thermal ellipsoid probabilities. Note that this view is down from the cap (O1B) of the monocapped square antiprism coordination polyhedron; O2B, O2C, O1D, O3AA and O2A, O1C, O2D, O1A form the upper and bottom square planes, respectively.

(25) Riley, P. E.; Abu-Dari, K.; Raymond, K. N. *Inorg. Chem.* **1983**, *22*, 3940.
(26) Kepert, D. L. In *Stereo-Inorganic Chemistry*; Jørgensen, C. K., Lappert, M. F., Lippard, S. J., Margrave, J. L., Niedenzu, K., Nöth, H., Parry, R. W., Yamatera, H., Eds.; Springer-Verlag: Berlin, 1982; pp 180−220.
(27) Xu, J.; Ziegler, M.; Raymond, K. N. Manuscript in preparation.
(28) Piyamongkol, S.; Liu, Z. D.; Hider, R. C. *Tetrahedron* **2001**, *57*, 3470−3486.
(29) SMART Area Detector Software Package; Siemens Industrial Automation, Inc., Madison, WI, 1995.
(30) SAINT: SAX Area-Detector Integration Program (V.4.024), Siemens Industrial Automation, Inc., Madison, WI, 1995.
(31) SADABS: Siemens Area Detector ABSsorption correction program, Sheldrick, G., 1996.
(32) Sheldrick, G. M. *Acta Crystallogr.* **1990**, *A46*, 467.
(33) Sheldrick, G. M. *SHELXTL-97, Program for the Refinement of Crystal Structures*; University of Göttingen: Göttingen, Germany.
(34) Flack, H. D. *Acta Crystallogr.* **1983** *A39*, 876.
(35) Harris, W. R.; Raymond, K. N.; Weitl, F. L. *J. Am. Chem. Soc.* **1981**, *103*, 2667−2675.
(36) Kappel, M.; Raymond, K. N. *Inorg. Chem.* **1982**, *21*, 3437−3442.
(37) Whisenhunt, D. W., Jr.; Neu, M. P.; Hou, Z.; Xu, J.; Hoffman, D. C.; Raymond, K. N. *Inorg. Chem.* **1996**, *35*, 4128.

Table 3. X-ray Crystallographic Information for Pr-Me-3,2-HOPO (HL^2) and $[Th(L^2)_4]\cdot H_2O$

compound	HL^2	$[Th(L^2)_4]\cdot H_2O$
empirical formula	$C_{13}H_{18}N_2O_3$	$ThC_{40}H_{52}N_8O_{12}\cdot H_2O$
fw	210.23	1086.95
cryst syst	triclinic	orthorhombic
space group	$P\bar{1}$ (No. 2)	$Pna2_1$ (No. 33)
T, °C	−139(2)	−112(2)
a, Å	8.1492(7)	17.1250(5)
b, Å	11.1260(9)	12.3036(7)
c, Å	23.402(2)	23.880(1)
α, deg	87.569(1)	90
β, deg	86.592(1)	90
γ, deg	87.480(1)	90
V, Å^3	2114.3(3)	5031.6(4)
Z	8	4
ρ_{calcd}, g cm^{-3}	1.321	1.435
λ, Å	0.71072	0.71072
abs coeff, cm^{-1}	0.99	30.27
2θ range, deg	$3.48 < 2\theta < 46.56$	$5.32 < 2\theta < 46.62$
no. of unique data	5452	6388
params (restraints)	541(0)	474(1)
R1[a] [$I > 2\sigma(I)$]	0.065	0.0477
wR2[b] [$I > 2\sigma(I)$]	0.1322	0.0678

[a] $R1 = \sum||F_o| - |F_c||/\sum|F_o|$. [b] $wR2 = \{\sum[w(F_o^2 - F_c^2)^2]/\sum[w(F_o^2)^2]\}^{1/2}$.

Table 4. Selected Bond Distances (Å) and Angles (deg) for HL^2

	Distances		
O(1)−C(2)	1.262(4)	C(2)−C(3)	1.427(5)
O(2)−C(3)	1.359(4)	C(3)−C(4)	1.367(5)
O(3)−C(7)	1.241(4)	C(4)−C(5)	1.425(5)
N(1)−C(2)	1.371(4)	C(4)−C(7)	1.500(5)
N(1)−C(6)	1.373(4)	C(5)−C(6)	1.334(5)
N(2)−C(7)	1.337(4)		
	Angles		
O(1)−C(2)−N(1)	120.1(3)	C(3)−C(4)−C(5)	117.7(3)
O(1)−C(2)−C(3)	123.1(3)	C(3)−C(4)−C(7)	125.4(3)
O(2)−C(3)−C(4)	121.8(3)	C(6)−C(5)−C(4)	120.7(3)
O(2)−C(3)−C(2)	116.3(3)	C(5)−C(4)−C(7)	116.9(3)
O(3)−C(7)−N(2)	121.4(3)	C(5)−C(6)−N(1)	121.1(3)
O(3)−C(7)−C(4)	119.7(3)	N(2)−C(7)−C(4)	118.9(3)
N(1)−C(2)−C(3)	116.8(3)	C(2)−N(1)−C(6)	121.8(3)
C(4)−C(3)−C(2)	121.9(3)	C(7)−N(2)−C(8)	121.8(3)

X-ray Crystal Structures. In order to compare the structure of the free ligand to Th(IV)-coordinated ligand, an X-ray crystal diffraction study was carried out for the bidentate ligand HL^2. The ligand crystallizes in the triclinic space group $P\bar{1}$ with $Z = 8$. The data collection and crystallographic parameters are summarized in Table 3, and the selected bond distances and angles are given in Table 4. A structural diagram of HL^2 (Figure 3) clearly demonstrates that this free ligand is predisposed for complexation.

It is important to note that in the free ligand the amide nitrogen atom forms a strong hydrogen bond with the adjacent phenolic oxygen atom (average $N_{amide}-O_{phenolic} = 2.68$ Å); the phenolic proton also forms a hydrogen bond with the adjacent oxo oxygen atom (average $O_{oxo}-O_{phenolic} = 2.72$ Å). This hydrogen bond scheme enforces a coplanar arrangement of HOPO ring and the amide moiety; the same ligand geometry has been observed in all crystal structures of the Me-3,2-HOPO−metal complexes to date.[17,19,22] Unlike catecholamides or 2,3-dihydroxyterephthalamides, no 180° rotation of the amide group accompanies metal complexation;[24] so for the Me-3,2-HOPO compounds, the uncomplexed and complexed ligands share the same conformation.

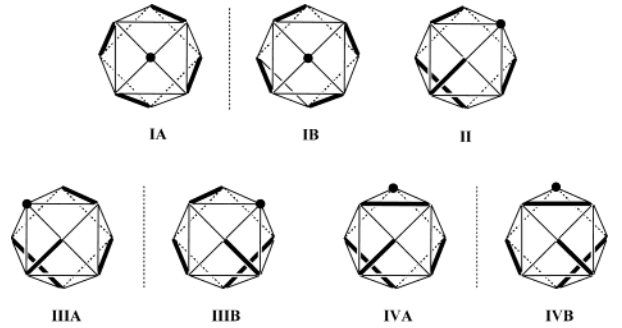

Figure 5. The seven possible coordination geometries of [M(bidentate)$_4$(monodentate)] complexes.

Table 5. Selected Bond Distances (Å) and Angles (deg) for $Th(L^2)_4\cdot 0.5H_2O$

	Distances		
Th(1)−O(1A)	2.507(5)	N(1A)−C(2A)	1.382(11)
Th(1)−O(1B)	2.433(11)	N(1A)−C(6A)	1.410(9)
Th(1)−O(1C)	2.606(8)	N(2A)−C(7A)	1.345(11)
Th(1)−O(1D)	2.553(17)	N(2A)−C(8A)	1.414(13)
Th(1)−O(2A)	2.448(5)	C(2A)−C(3A)	1.408(12)
Th(1)−O(2B)	2.261(8)	C(3A)−C(4A)	1.409(10)
Th(1)−O(2C)	2.373(6)	C(4A)−C(5A)	1.412(9)
Th(1)−O(2D)	2.541(11)	C(4A)−C(7A)	1.468(11)
Th(1)−O(3AA)	2.381(6)	C(5A)−C(6A)	1.354(10)
O(1A)−C(2A)	1.312(8)	C(7A)−O(3AB)	1.359(15)
O(2A)−C(3A)	1.281(9)		
	Angles		
O(2A)−Th(1)−O(1A)	63.93(16)	O(2B)−Th(1)−O(3AA)	92.7(7)
O(2B)−Th(1)−O(1B)	68.0(3)	O(2B)−Th(1)−O(2C)	94.9(6)
O(2C)−Th(1)−O(1C)	59.2(6)	O(2C)−Th(1)−O(1D)	83.2(6)
O(2D)−Th(1)−O(1D)	61.9(5)	O(3AA)−Th(1)−O(1D)	70.9(6)
O(3AA)−Th(1)−O(1A)	78.17(19)	O(2C)−Th(1)−O(3AA)	147.3(2)
O(3AA)−Th(1)−O(2D)	63.0(7)	O(2B)−Th(1)−O(1D)	140.3(4)
O(3AA)−Th(1)−O(1B)	76.5(6)	O(1A)−Th(1)−O(1C)	108.1(5)
O(1B)−Th(1)−O(1D)	73.0(2)	O(2A)−Th(1)−O(2D)	97.7(5)
O(2C)−Th(1)−O(1B)	77.0(5)	O(1B)−Th(1)−O(1A)	132.8(6)
O(2A)−Th(1)−O(1C)	69.2(4)	O(1B)−Th(1)−O(2A)	134.7(5)
O(2D)−Th(1)−O(1C)	63.2(3)	O(1B)−Th(1)−O(1C)	119.1(4)
O(1A)−Th(1)−O(2D)	72.6(6)	O(1B)−Th(1)−O(2D)	126.5(4)

The thorium complex crystallizes in the polar space group $Pna2_1$ (No. 33); there are four $[Th(L^2)_4]\cdot H_2O$ formula units in the unit cell (for crystallographic data see Table 3). An ORTEP diagram of the complex is shown in Figure 4, and selected bond distances and angles are given in Table 5. Each thorium is nine coordinated by four bidentate ligands and by a fifth ligand moiety of a neighboring thorium complex through its amide oxygen. The linkage of adjacent $[Th(L^2)_4]$ units generates a one-dimensional chain structure. Consistent with other Me-3,2-HOPO complexes, the average metal−phenolic oxygen bond length is slightly shorter than that of oxo oxygen.[17,19,23] The average distance of $Th-O_{phenolic}$ is 2.405(8) Å, close to that of 2.403(3) Å observed in the 1,2-HOPO analogue, tetrakis(1-oxy-2-pyridonato)-aqua-thorium-(IV),[25] while the average distance of $Th-O_{oxo}$ is 2.524(11) Å, a little longer than that of 2.476(4) Å in the 1,2-HOPO analogue. The average bite angle of complexation is 63.2-(4)°, similar to that of 63.9(1)° in the 1,2-HOPO analogue.[25]

The central thorium atom is nine coordinate. Repulsion energy calculations predict that the monocapped square-antiprism geometry is more stable than other possible geometries for [M(bidentate)$_4$(monodentate)] complexes.[26] The possible arrangements of four equivalent bidentate

ligands coordinated to a metal ion with a monocapped square-antiprism geometry are shown in Figure 5. The heavy edge connects two sites occupied by the bidentate chelates, while the black dot indicates the site occupied by the monodentate ligand. Note that **II** is symmetric while **IA**/**IB**, **IIIA**/**IIIB**, and **IVA**/**IVB** are pairs of enantiomers. However, this is true only for symmetrical bidentate ligands (such as catechol), and not for asymmetrical ligands such as HOPOs. A full analysis of the number of possible isomers for the asymmetrical bidentate ligand situation will be discussed elsewhere.[27] Kepert has discussed the monocapped square-antiprism geometry of [M(bidentate)$_4$(monodentate)] complexes and suggested **IA**, **II**, **IIIA**, and **IVA** as the four possible geometries.[26] Indeed the coordination geometry of [Th(**L**^{2})$_4$]·H$_2$O presented in Figure 4 is best described as a slightly distorted monocapped square antiprism with the chelate arrangement represented by **IIIA** (Figure 5), alternatively with **IIIB** in the glide generated chain. The thorium atom is bound to nine oxygen donor atoms in a slightly distorted monocapped square-antiprismatic geometry. For the complex illustrated in Figure 4, one oxygen atom (O1B) occupies the cap site, while O2B, O2C, O1D, and O3AA, the amide oxygen donor from a neighboring thorium complex, form the upper square plane. The lower square plane is formed by O2A, O1C, O2D, and O1A. The rms deviation from the least squares plane of O2A, O1C, O2D, and O1A is 0.069; while the rms deviation from the least squares plane of O2B, O2C, O1D, and O3AA is 0.12. The angle between the two planes is 8.26°, deviating from 0° for an ideal monocapped square antiprism, and the twist angles are 40.5°, 47.1°, 45.2°, and 55.1° giving an average of 47.0°, close to the ideal value of 45°.

We recently presented a general definition of the shape measure (*S*), to describe and compare the geometry of eight-coordinate complexes.[19] Shape measure is defined as

$$S = \min\left[\sqrt{\frac{1}{m}\sum_{i=1}^{m}(\delta_i - \theta_i)^2}\right]$$

where m is the number of edges of the coordination polyhedron, δ_i is the observed dihedral angle along the ith edge of δ (angle between normals of adjacent faces), θ_i is the same angle of the corresponding ideal polytopal shape θ, and min is the minimum of all possible values. The calculation of shape measure can be extended to evaluate the geometry of a complex of any other coordination number. A generalized program for these calculations will be described elswhere.[27]

In the case of nine-coordinate complexes, there are five possible polyhedra: the tricapped trigonal prism, monocapped square antiprism, monocapped cube, tridiminished icosahedron, and triangular cupola.[26] The latter three (especially the last two) polyhedra have prohibitively high repulsion energies and are therefore not common.[26] For the complex [Th(**L**^{2})$_4$]·H$_2$O the shape measure for idealized monocapped square antiprism [$S(C_{4v}) = 7.72°$] is much lower than that of tricapped trigonal prism [$S(C_{2v}) = 9.10°$] and

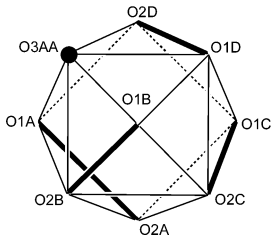

Figure 6. The coordination polyhedron of [Th(**L**^{2})]·H$_2$O, as viewed down the cap of the Archimedean antiprism. Note that the coordination polyhedron shares the same view with that in Figure 4.

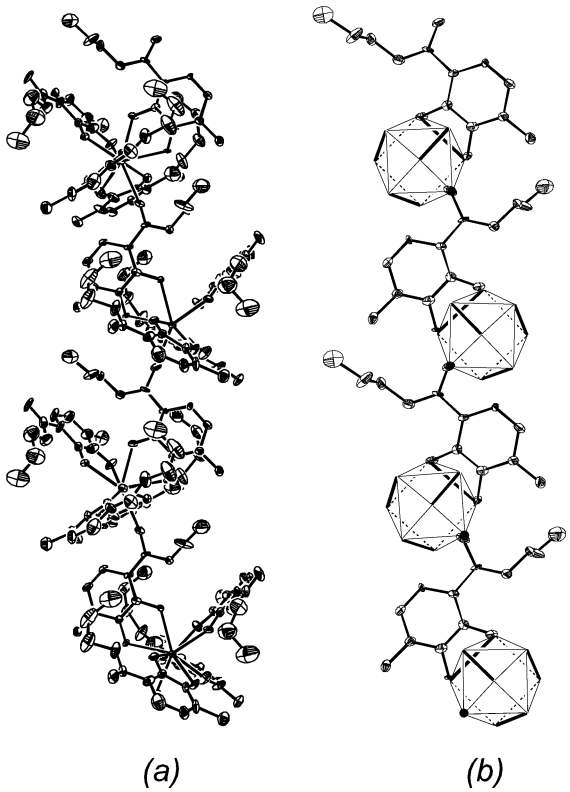

Figure 7. (a) Structure of part of the [Th(L^2)$_4$)]·H$_2$O linear coordination polymer. (b) A simplified structure of view a showing only the linking moieties and the coordination polyhedra of the linear coordination polymer.

monocapped cube [$S(C_{4v}) = 20.76°$]. The lower shape measure for the monocapped square antiprism C_{4v} clearly shows that the coordination polyhedron is closest to an idealized monocapped square antiprism.

In the unit cell of [Th(**L**^{2})$_4$]·H$_2$O, each thorium complex is connected to its enantiomeric neighbor via coordination of an amide oxygen to give a nine-coordinate complex. This results in an unusual linear coordination polymer composed of enantiomers **IIIA** and **IIIB**, which alternate to form a zigzag structure as shown in Figure 7. However, the simplicity of the NMR spectra of the complex in DMSO solution at room temperature confirms that the complex exists as discrete molecules in solution, presumably with a solvent molecule replacing the coordination site occupied by the amide oxygen in the solid state.

Conclusions

The bidentate ligands PR-1,2-HOPO (H**L**^{1}), PR-Me-3,2-HOPO (H**L**^{2}), and PR-3,4-HOPO-N (H$_2$**L**^{3}) form very stable

complexes with Th(IV) in aqueous solution, giving overall formation constants (log β_{140}) of 36.0(3), 38.3(3), and 41.8(5), respectively. The different acidities of these ligands (log K_a of 4.96(2), 6.12(1) for H**L**^{1}, H**L**^{2}; log K_{a1} and log K_{a2} of 9.47(2) and 3.03(4) for H**L**^{3}, respectively) lead to significantly different complexation behavior as a function of pH. From the species distribution diagram (Figure 1), one can find that the fully complexed species is the dominant species in acid (pH < 6) for H**L**^{1}, in weak acid to physiological pH for H**L**^{2}, and at high pH (>8) for H**L**^{3}. These differences in chemical properties of the bidentate hydroxypyridinonate could be utilized in the design and synthesis of multidentate HOPO ligands with varying chemical properties for actinide sequestration in vivo and environment applications. While attachment of the 1,2- and 3,2-ligands to make multidentate ligands is now straightforward, previously synthesized 3,4-HOPO-N ligands do not have the proper coordination geometry,[7,8] although a new synthetic approach to such multidentate 3,4-HOPO ligands has been recently reported.[28]

A comparison of the structure of Th(**L**^{2})$_4$·H_2O with that of H**L**^{2} reveals that the ligand geometry in both the free ligand and the metal complex is essentially identical. The hydrogen bonds between the amide nitrogen and the proximal phenolic oxygen enhance the rigidity in both structures and demonstrate that the Me-3,2-HOPO ligands are predisposed for metal chelation. In the crystal of [Th(**L**^{2})$_4$]·H_2O, the complex forms an unusual linear coordination polymer in which enantiomers **IIIA** and **IIIB** alternate to form a zigzag structure (Figure 7).

Experimental Section

All chemicals were used as received from Aldrich unless otherwise noted. 1-Benzyloxy-2(1*H*)-pyridinone-6-carboxylic acid (1,2-HOPOBn acid **1**),[9] 3-benzyloxy-1-methyl-2(1*H*)-pyridinone-4-carboxylic acid (Me-3,2-HOPOBn acid **4**),[10] and 3-benzyloxy-2-methyl-4(1*H*)-pyridinone-*N*-acetic acid (3,4-HOPO-N acid **7**)[11] were prepared by published methods. ^{1}H NMR and ^{13}C NMR spectra were obtained on Bruker AMX-300, AMX-400 or DRX-500 spectrometers and are reported in parts per million. Ultraviolet/visible spectra were recorded on a Hewlett-Packard 8450A diode array spectrophotometer. Th(acac)$_4$ was purchased from Bodman Chemicals. $ThCl_4$·$3H_2O$ (99.9%) was from ROC/RIC and was dissolved in H_2O to make solutions ~0.05 M in Th(IV). The solutions were standardized with Na_2EDTA (0.0997 M Aldrich) using pyrocatechol violet as an indicator. Elemental (CHN) analyses were performed at the Elemental Analysis Facility, College of Chemistry, University of California, Berkeley.

Syntheses. 1-Benzyloxy-2(1*H*)-pyridinone-6-carboxylic Acid Propylamide (PR-1,2-HOPOBn) (3). To a suspension of 1,2-HOPOBn acid (**1**, 1.0 g, 4 mmol) in toluene (50 mL) was added excess oxalyl chloride (1.0 g) with stirring. Gas bubbles evolved and the suspension turned clear upon the addition of a drop of DMF as a catalyst. The mixture was warmed to 50° C for 4 h, and the solvent was removed under reduced pressure to leave the raw acid chloride as a pale yellow oil. The oil was dissolved in methylene chloride (30 mL), and excess propylamine (0.4 g, 6.7 mmol) was added with stirring. The solution was extracted with 0.5 M HCl solution and saturated NaCl solution successively, and the organic phase was loaded onto a flash silica column. Elution with 2−6% methanol in methylene chloride allowed separation of compound **3** as white foam, yield 90%. ^{1}H NMR (500 MHz, $CDCl_3$): δ 0.75 (t, 3H, J = 7.5 Hz, CH_3), 1.39 (q, 2H, J = 7.3 Hz, CH_2), 3.08 (q, 2H, J = 6.7 Hz, CH_2), 5.10 (s, 2H, CH_2), 6.13 (dd, 1H, J = 6.5 Hz, 1.5 Hz, arom H), 6.32 (dd, 1H, J = 9.5 Hz, 1.5 Hz, arom H), 7.02 (dd, 1H, J = 9.0 Hz, 7.0 Hz, arom H), 7.17−7.29 (m, 5H, arom H), 7.66 (t, 1H, J = 5.7 Hz, amid H). ^{13}C NMR (100 MHz, $CDCl_3$): δ 11.0, 21.9, 41.3, 78.6, 105.3, 122.5, 128.0, 128.7, 129.4, 133.0, 137.9, 143.0, 158.2, 160.0. MS(+FAB): 287.2 (MH^+).

1-Hydroxy-2(1*H*)-pyridinone-2-carboxylic Acid Propylamide (PR-1,2-HOPO) (HL^{1}). Compound **3** (1.0 g, 3.5 mmol) was dissolved in 25 mL of a 1:1 mixture of concentrated HCl and acetic acid. The mixture was stirred for 36 h, and the solvent was removed under vacuum. The residue was washed with diethyl ether and dried in a vacuum oven at 70 °C for 6 h. A beige solid was obtained as product, yield 85%.

^{1}H NMR (500 MHz, $CDCl_3$): δ 0.87 (t, 3H, J = 7.2 Hz, CH_3), 1.47 (q, 2H, J = 7.2 Hz, CH_2), 3.14 (q, 2H, J = 6.5 Hz, CH_2), 6.25 (d, 1H, J = 7.0 Hz, arom H), 6.55 (d, J = 9.0 Hz, 1H, arom H), 7.38 (d, 1H, J = 8.0 Hz, arom H), 8.75 (s, br, 1H, amid H). ^{13}C NMR (100 MHz, $CDCl_3$): δ 11.4, 22.1, 40.7, 103.6, 119.2, 137.4, 142.5, 157.5, 160.3. Anal. Calcd (found) for $C_9H_{12}N_2O_3$·H_2O: C, 50.46 (50.73); H, 6.58 (6.65); N, 13.07 (12.88). MS-(+FAB): 197.2 (MH^+).

3-Benzyloxy-1-methyl-2(1*H*)-pyridinone-4-Carboxylic Acid Propylamide (PR-Me-3,2-HOPOBn) (6). To a suspension of 3-benzyloxy-1-methyl-2(1*H*)-pyridinone-4-carboxylic acid (**4**, 2.59 g, 10 mmol) in benzene (25 mL) was added excess oxalyl chloride (1.65 g, 26 mmol). Vigorous gas evolution was observed after a drop of dimethylformamide (DMF) was added as catalyst, and the turbid solution turned clear and was then heated to 50 °C for 4 h. Solvent was removed under reduced pressure, and the residue was dissolved in a solution of propylamine (0.71 g, 12 mmol) in dry methylene chloride (20 mL). A silica gel plug as described in the synthesis of **3** was used to purify this solution, and a white foam was obtained as product after removal of the solvent; yield 2.92 g, 94%.

^{1}H NMR (300 MHz, $CDCl_3$): δ 0.79 (t, 3H, J = 7.4 Hz, CH_3), 1.33 (q, 2H, J = 7.2 Hz, CH_2), 2.95 (q, 2H, J = 6.5 Hz, CH_2), 3.18 (s, 3H, CH_3), 5.38 (s, 2H, benzyl CH_2), 6.81 (d, 1H, J = 7.2 Hz, arom H), 7.12 (d, 1H, J = 7.2 Hz, arom H), 7.30−7.50 (m, 5H, arom H), 7.92 (t, J = 5.6 Hz, 1H, amid H). ^{13}C NMR (100 MHz, $CDCl_3$): δ 11.4, 20.1, 37.7, 41.5, 74.9, 105.0, 128.7, 128.8, 129.0, 130.6, 132.0, 146.5, 159.7, 163.0. Anal. Calcd (found) for $C_{17}H_{20}N_2O_3$·H_2O: C, 64.13 (64.01); H, 6.96 (6.71); N, 8.80 (8.79). MS(+FAB): 301.4 (MH^+).

3-Hydroxy-1-methyl-2(1*H*)-pyridinone-4-Carboxylic Acid Propylamide (PR-Me-3,2-HOPO) (HL^{2}). PR-Me-3,2-HOPOBn (**6**, 2.00 g, 6.66 mmol) and 10% Pd/C catalyst (200 mg) were suspended in methanol (50 mL). The mixture was stirred overnight under hydrogen (1 atm). The catalyst was removed by filtration, the filtrate was evaporated to dryness, and the residue was recrystallized from a methanol−ether mixture to afford white crystals, yield 1.28 g, 92%. ^{1}H NMR (300 MHz, DMSO-d_6): δ 0.88 (t, 3H, J = 7.4 Hz, CH_3), 1.52 (q, 2H, J = 7.2 Hz, CH_2), 3.23 (q, 2H, J = 6.6 Hz, CH_2), 3.46 (s, 3H, CH_3), 6.52 (d, J = 7.1 Hz, 1H, arom H), 7.18 (t, J = 7.2 Hz, 1H, arom H), 8.46 (t, J = 5.6 Hz, 1H, amide H). ^{13}C NMR (100 MHz, $CDCl_3$): δ 11.3, 22.2, 36.8, 40.8, 102.4, 117.0, 127.7, 147.9, 158.0, 165.6. Anal. Calcd (found) for $C_{10}H_{14}N_2O_3$: C, 57.13 (57.44); H, 6.71 (6.63); N, 13.32.-(13.25). MS(+FAB): 211.1 (MH^+).

3-Benzyloxy-2-methyl-4(1*H*)-pyridinone-*N*-acetic Acid Propylamide (9). To a solution of 3-benzyloxy-2-methyl-4(1*H*)-pyridinone-*N*-acetic acid (**7**, 2.0 g, 7.3 mmol) and *N*-hydroxysuccin-

imide (NHS) (0.9 g, 7.8 mmol) in dry pyridine (50 mL) was added 1,3-dicyclohexylcarbodiimide (DCC) (1.5 g, 7.3 mmol). The solution was stirred for 4 h, and *n*-propylamine (0.74 g, 10 mmol) was added. The mixture was stirred for an additional 4 h and filtered to remove the solid of dicyclohexylurea (DCU); and the solvent was removed from the filtrate by rotary evaporation. The residue was taken up in a minimal amount of methylene chloride and extracted with 0.5 M NaOH and 0.5 M HCl successively. Evaporation of the methylene chloride solution gave compound **9** as a beige crystalline solid (1.40 g, 60.6%). ^{1}H NMR(500 MHz, $CDCl_3$): δ 0.82 (tt, 3H, J = 7.3 Hz, CH_3), 1.45 (qq, 2H, J = 7.3 Hz, CH_2), 2.07 (s, 3H, CH_3), 3.10 (s, br, 2H, CH_2), 4.45 (s, 2H, CH_2), 4.97 (s, 2H, CH_2), 6.52 (dd, 1H, J = 7.5 Hz, 3 Hz, arom H), 7.11 (dd, 1H, J = 7.5 Hz, 1.5 Hz, arom H), 7.20 (m, 3H, arom H), 7.25−7.32 (m, 2H, arom H), 8.73 (t, 1H, J = 5.3 Hz, amide H). ^{13}C NMR (100 MHz, $CDCl_3$): δ 11.2, 12.3, 22.3, 41.1, 55.5, 72.8, 116.2, 127.7, 127.8, 128.1, 136.9, 140.2, 142.9, 145.5, 165.7, 173.1. Anal. Calcd (found) for $C_{18}H_{22}N_2O_3 \cdot 0.5\ H_2O$: C, 66.85 (66.90); H, 7.16 (6.82); N, 8.66 (8.75). MS(+FAB): 315.2 (MH^+).

3-Hydroxy-2-methyl-4(1*H*)-pyridinone-*N*-acetic Acid Propylamide (PR-3,4-HOPO-N, HL^3). Compound **9** (1 g, 3.2 mmol) was deprotected by the catalytic hydrogenation procedure mentioned above. Pure product was obtained as a white solid (0.63 g, 87%). ^{1}H NMR (500 MHz, DMSO-d_6): δ 0.82 (t, 3H, J = 7.2 Hz, CH_3), 1.15 (hex, 2H, J = 7.2 Hz, CH_2), 2.35 (s, 3H, CH_3), 3.04 (q, 2H, J = 6.5 Hz, CH_2), 5.18 (s, 2H, CH_2), 7.37 (d, 1H, J = 7.0 Hz, arom H), 8.23 (d, J = 7.0 Hz, 1H, arom H), 8.84 (t, J = 5.5 Hz, 1H, amide H). ^{13}C NMR (125 MHz, DMSO-d_6): δ 11.4, 12.6, 22.2, 40.7, 57.9, 110.4, 139.7, 142.2, 142.6, 159.3, 164.7. Anal. Calcd (found) for $C_{11}H_{16}N_2O_3$: C, 58.91 (58.82); H, 7.19 (7.31); N, 12.49 (12.34). MS(+FAB): 225.3 (MH^+).

[Th(L^1)$_4$]·2H$_2$O. To a solution of Th(acac)$_4$ (63 mg, 0.10 mmol) was added H**L^1** (98 mg, 0 45 mmol) in dry methanol (10 mL) with stirring. The mixture was heated at reflux under N_2 overnight. The solvent was removed under reduced pressure, and the residue was taken up into chloroform (20 mL). The chloroform solution was washed with saline (3 × 10 mL). After drying with magnesium sulfate, the chloroform was removed to give the product as a beige solid, yield 75 mg (71%). ^{1}H NMR (300 MHz, DMSO-d_6): δ 0.79 (t, 12H, J = 7.4 Hz, CH_3), 1.35 (q, 8H, J = 7.2 Hz, CH_2), 3.20 (q, 8H, J = 6.5 Hz, CH_2), 6.79 (d, 4H, J = 7.8 Hz, arom H), 7.39 (t, 4H, J = 7.9 Hz, arom H), 7.50 (d, 4H, J = 6.8 Hz, arom H), 9.92 (s, br, 4H, amide H). Anal. Calcd (found) for $ThC_{36}H_{44}N_8O_{12} \cdot 2H_2O$: C, 41.22 (41.13); H, 4.61 (4.81); N, 10.68 (10.49). MS-(+FAB): 1013.4 [Th(L^1)$_4$H$^+$].

[Th(L^2)$_4$]·2.5H$_2$O. A solution of Th(acac)$_4$ (63 mg, 0.10 mmol) in dry acetonitrile (10 mL) was added slowly to a stirred solution of H**L^2** (89 mg, 0 42 mmol) in acetonitrile (20 mL). The transparent solution turned turbid after a few minutes. The mixture was heated at reflux under N_2 overnight, during which time the complex was deposited as a beige fluffy precipitate. After cooling, it was collected by filtration, rinsed with cold acetonitrile, and dried under vacuum, yield 98 mg (0.088 mmol, 88% based on Th(acac)$_4$). ^{1}H NMR (300 MHz, DMSO-d_6): δ 0.66 (t, 12H, J = 7.4 Hz, CH_3), 1.15 (q, 8H, J = 7.2 Hz, CH_2), 2.95 (q, 8H, J = 6.5 Hz, CH_2), 3.48 (s, 12H, CH_3), 6.81 (d, 4H, J = 7.1 Hz, arom H), 6.94 (d, 4H, J = 7.2 Hz, arom H), 9.39 (t, 4H, J = 5.6 Hz, amide H). Anal. Calcd (found) for $ThC_{40}H_{52}N_8O_{12} \cdot 2.5\ H_2O$: C, 43.12 (43.13); H, 5.15 (4.91); N, 10.05 (9.79). MS(+FAB): 1069.7 [Th(L^2)$_4$H$^+$], 859.3 [Th(L^2)$_3^+$].

[Th(L^3)$_4$]·2.5H$_2$O. A solution of Th(acac)$_4$ (63 mg, 0.10 mmol) in dry methanol (20 mL) was added to H**L^3** (99 mg, 0.44 mmol) in dry methanol with stirring. The mixture was heated at reflux under N_2 overnight and then diluted with methylene chloride (80 mL). The mixed solution was passed through a silica gel plug, and the plug was eluted with 20% methanol in methylene chloride. The combined eluents were evaporated to dryness to afford a beige solid as product, yield 65%. ^{1}H NMR (500 MHz, CD_3OD): δ 0.92 (t, 12H, J = 7.2, CH_3), 1.53 (q, 8H, J = 7.2, CH_2), 2.28 (s, 12H, CH_3), 3.17 (q, 8H, J = 6.2 Hz, CH_2), 4.83 (s, br, 8H, NCH_2), 6.39 (s, br, 4H, arom H), 7.55 (s, br, 4H, arom H). Anal. Calcd (found) for $ThC_{44}H_{60}N_8O_{12} \cdot 2.5\ H_2O$: C, 45.16 (45.07); H, 5.59 (5.61); N, 9.57 (9.69). MS(+FAB): 1125.5 [Th(L^3)$_4$H$^+$].

X-ray Crystallography. Colorless rhomboid crystals of PR-Me-3,2-HOPO and colorless thin plates of Th(PR-Me-3,2-HOPO)$_4$ were grown by diffusion of ethyl ether into a solution of the complex in methanol. Selected crystals were mounted in Paratone N oil on the ends of quartz capillaries and frozen into place under a low-temperature nitrogen stream. Data were collected on a Siemens SMART/CCD X-ray diffractometer[29] with Mo Kα radiation (λ = 0.71072 Å). Intensity data, to a maximum 2θ range of 46.62°, were extracted from the frames using the program SAINT[30] with box parameters of 1.6 × 1.6 × 0.6. The data were corrected for Lorentz and polarization effects, and an empirical absorption correction was applied using the SADABS[31] program. No decay correction was applied. The structures were solved by direct methods using SHELXS-97.[32] Full-matrix least squares refinements based on F^2 were performed in SHELXTL-97.[33] In the structure of PR-Me-3,2-HOPO (H**L^2**), all non-hydrogen atoms were refined anisotropically. Hydrogen atoms were assigned to idealized positions. Crystallographic information is summarized in Table 3.

Since the crystal of Th(**L^2**)$_4$·H$_2$O was a very thin plate (0.50 × 0.14 × 0.008 mm), it was mounted on top of and perpendicular to a quartz capillary with the aid of N-paratone oil. Surface tension caused a slight bending of the crystal, which could contribute to the difficulty in solving the structure. The orientation of the polar crystal was established based on a comparison of F_o and F_c for reflections of Friedel mates (Flack factor 0.00).[34] Most of the non-hydrogen atoms were refined using anisotropic thermal displacement parameters, except the carbon atoms of the propyl moieties due to the oblate or prolate thermal ellipsoid with big thermal motions. Hydrogen atoms in the complex were placed at calculated positions riding on their parameters. Crystallographic data (excluding structure factors) for the structures reported in this paper have been deposited in the Cambridge Crystallographic Data Center with CCDC numbers 160035 and 160036.

Potentiometric Titrations. The apparatus and method used for potentiometric titrations have been described in detail elsewhere.[35,36] The solutions were maintained at a constant ionic strength (0.100 M KCl) and at a constant temperature of 25.0 ± 0.1 °C. The thermodynamic reversibility of each potentiometric titration was confirmed by carrying out titrations from acid to base and vice versa. The models used to fit the titration data were refined by the nonlinear least squares program BETA90.[36,37] All results presented here are the average of at least three separate titrations.

Spectrophotometric Titrations. The apparatus and method for spectrophotometric titrations have been described in detail elsewhere.[37] The solutions were maintained at a constant ionic strength (0.100 M KCl) and at a constant temperature 25.0 ± 0.1 °C (constant-temperature bath). The thermodynamic reversibility of each spectrophotometric titration was also confirmed by carrying out titrations from acid to base and vice versa (where possible). The models used to fit the titration data were refined by the nonlinear least squares program REFSPEC.[38] All results presented here are the average of at least three separate titration experiments.

Acknowledgment. This research was supported by the Director, Office of Energy Research, Office of Basic Energy Sciences, Chemical Sciences Division, U.S. Department of Energy, under Contract No. DE-AC03-76SF00098 and the National Institute of Environmental Health Sciences Grant No. ES02698. We thank Dr. C. Sunderland and Dr. F. J. Hollander for assistance with the X-ray diffraction studies. We would like to thank the referees for their invaluable suggestions.

(38) Turowski, P. N.; Rodgers, S. J.; Scarrow, R. C.; Raymond, K. N. *Inorg. Chem.* **1988**, *27*, 474−481.

Supporting Information Available: Figures of potentiometric titration curves, spectra, and component diagrams for H$\mathbf{L^1}$, H$\mathbf{L^3}$, and their thorium complexes. X-ray crystallographic files for H$\mathbf{L^2}$ and Th($\mathbf{L^2}$)$_4$·H_2O (CIF and PDF). This material is available free of charge via the Internet at http://pubs.acs.org.

IC0259888